

Suppression of Photocatalytic Activity of ZnO Fabricated by Sol-Gel Method under Gentle Vacuum Condition for Highly Durable Organic Solar Cells

Masahiro Nakano^{a*}, Tomoki Kobayashi^a, Masaki Kaneda^a, Sae Nakagawa^a, Md. Shahiduzzaman^b, Makoto Karakawa^{a,b,c}, Tetsuya Taima^{a,b,c}

^aGraduate School of Natural Science and Technology, Kanazawa University, Kakuma-machi, Kanazawa, Ishikawa 920-1192, Japan

^bNanomaterial Research Institute (NanoMaRI), Kanazawa University, Kakuma-machi, Kanazawa, Ishikawa 920-1192, Japan

^cInstitute for Frontier Science Initiative (InFiniti), Kanazawa University, Kakuma-machi, Kanazawa, Ishikawa 920-1192, Japan

Contents

1. Electrical resistance measurement of ZnO films
2. Water-contact angle measurement of ZnO films
3. Summarized photovoltaic properties
4. Changes of Photovoltaic properties with photo-irradiation time
5. Changes of R_{ZnO} with photo-irradiation time
6. Thermal stability testing of ZnO^{air}-based OSCs

1. Electrical resistance measurement of ZnO films

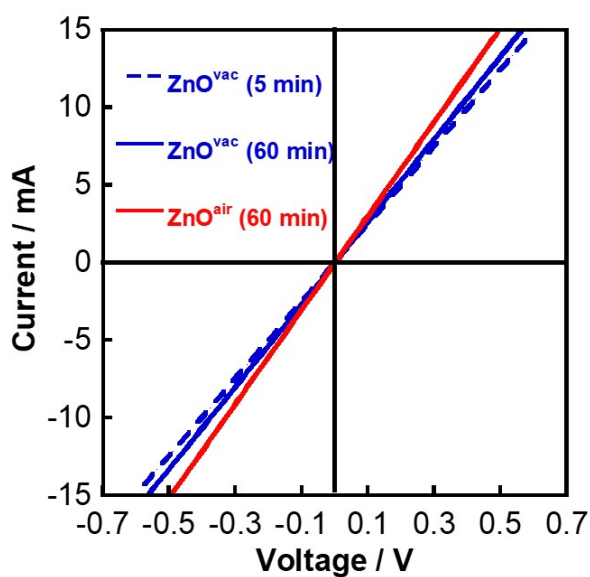


Figure S1. J - V characteristics of ZnO films sandwiched by ITO and Ag electrodes (ITO/ZnO/Ag).

2. Water-contact angle measurement of ZnO films

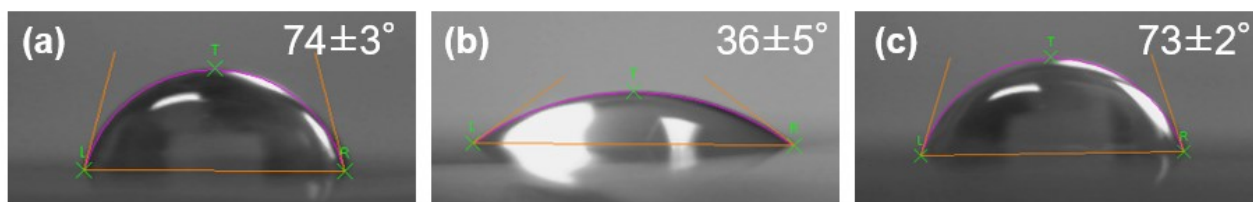


Figure S2. Water-contact angle measurement of ZnO^{vac} (a) and ZnO^{air} (b) prepared by 60 minutes of thermal annealing (100°C), ZnO^{vac} prepared by 5 minutes of thermal annealing (c).

3. Summarized photovoltaic properties

Table S1. Summary of photovoltaic properties of OSCs based on ZnO^{air} and ZnO^{vac}.

ZnO Preparation	J_{sc} / mAcm ⁻²	V_{oc} / V	FF	PCE / %
in air	9.1 (±0.2)	0.57 (±0.0)	0.61 (±0.0)	3.1 (±0.1)
under vacuum	9.0 (±0.3)	0.57 (±0.1)	0.61 (±0.1)	3.1 (±0.2)

4. Changes of Photovoltaic properties with photo-irradiation time

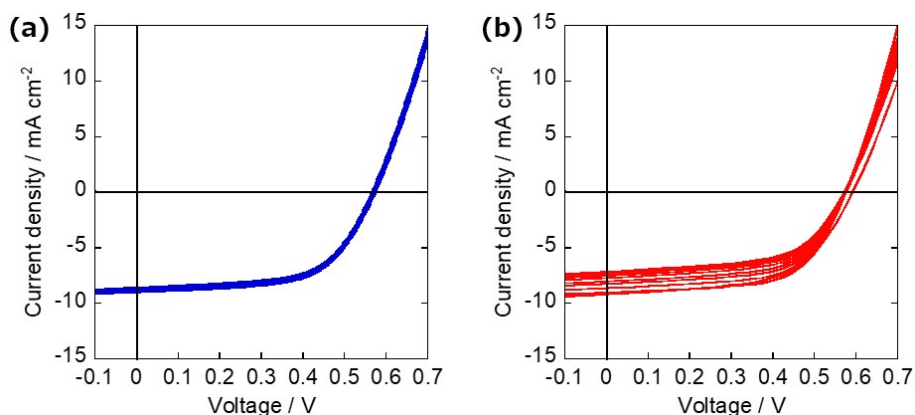


Figure S3. Changes in typical J - V characteristics of OSCs based on ZnO^{vac} (a) and ZnO^{air} (b) with photoirradiation time (0–100 h).

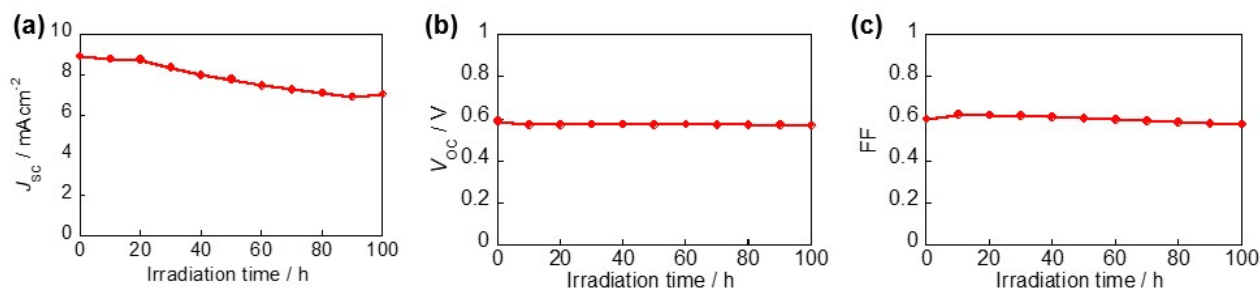


Figure S4. Changes in J_{sc} (a), V_{oc} (b), and FF (c) values with continuous photoirradiation of OSCs based on ZnO^{air} .

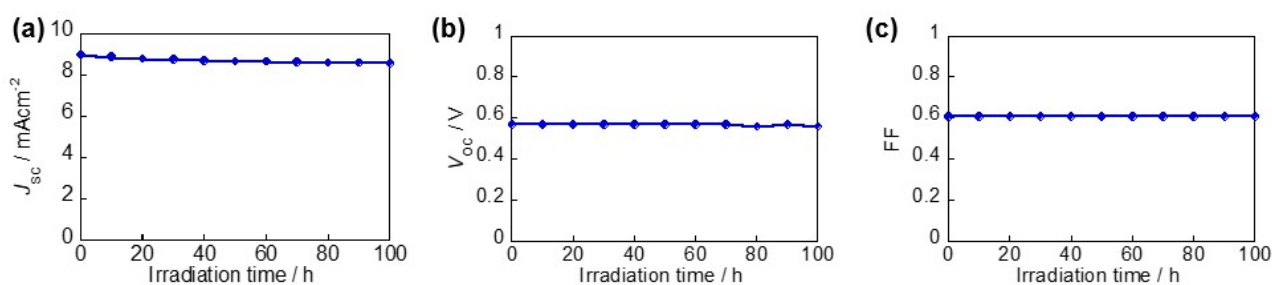


Figure S5. Changes in J_{sc} (a), V_{oc} (b), and FF (c) values with continuous photoirradiation of OSCs based on ZnO^{vac} .

5. Changes of R_{ZnO} with photo-irradiation time

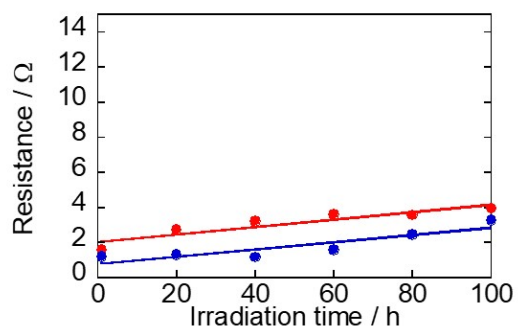


Figure S6. Changes in R_{ZnO} of OSCs based on ZnO^{vac} (blue trace) and ZnO^{air} (red trace) with photo-irradiation time (0–100 h).

6. Thermal stability testing of ZnO^{air}-based OSCs

The thermal stability of ZnO^{air}-based OSCs was investigated under dark conditions at 65°C which is similar temperature during continuous photoirradiation. The ZnO^{air}-based device showed good thermal stability; the PCE value of the ZnO^{air}-based OSC was kept 97% of the initial value after 50 h of thermal stability testing (Figure S7). Moreover, AC-impedance measurement of the ZnO^{air}-based device indicates that the active layer does not decompose by thermal heating without photo-irradiation (Figure S8). Considering the poor stability of ZnO^{air}-based devices under continuous photo-irradiation, the photo-degradation of active layer materials on ZnO^{air} should be caused by photo-catalytic reaction.

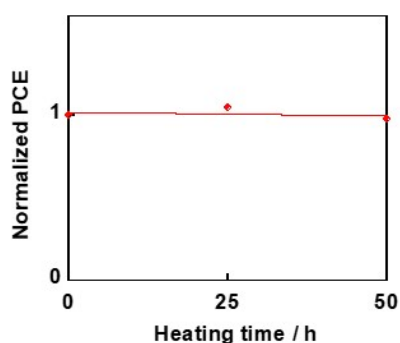


Figure S7. Changes of PCE of ZnO^{air}-based OSC under dark conditions at 65°C.

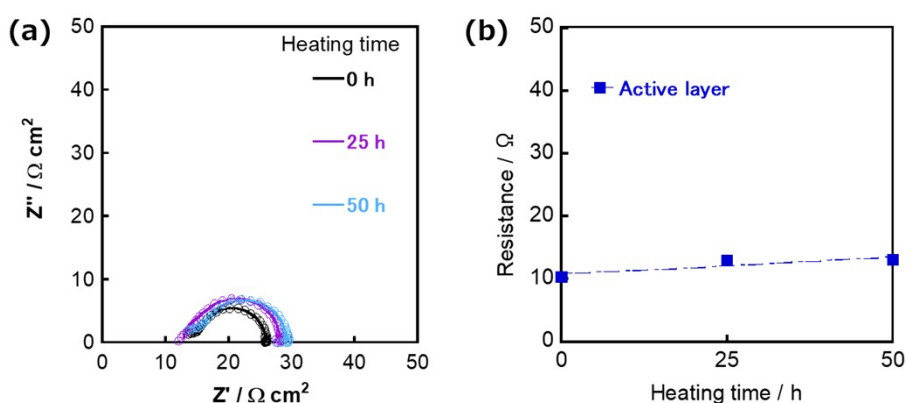


Figure S8. Nyquist plots of the ZnO^{air}-based OSC (a) and changes in resistance values of the active layer of the ZnO^{air}-based OSC with continuous thermal annealing (65°C) without photo-irradiation.